J Comput Aided Mol Des (2009) 23:705–714
DOI 10.1007/s10822-009-9294-z

Molecular dynamics simulation of S100B protein to explore ligand blockage of the interaction with p53 protein

Zhigang Zhou · Yumin Li

Received: 27 January 2009 / Accepted: 25 June 2009 / Published online: 14 July 2009

Abstract As a tumor suppressor, p53 plays an important role in cancer suppression. The biological function of p53 as a tumor suppressor is disabled when it binds to S100B. Developing the ligands to block the S100B-p53 interaction has been proposed as one of the most important approaches to the development of anti-cancer agents. We screened a small compound library against the binding interface of S100B and p53 to identify potential compounds to interfere with the interaction. The ligand-binding effect on the S100B-p53 interaction was explored by molecular dynamics at the atomic level. The results show that the ligand bound between S100B and p53 propels the two proteins apart by about 2 Å compared to the unligated S100B-p53 complex. The binding affinity of S100B and p53 decreases by ~8.5–14.6 kcal/mol after a ligand binds to the interface from the original unligated state of the S100B-p53 complex. Ligand-binding interferes with the interaction of S100B and p53. Such interference could impact the association of S100B and p53, which would free more p53 protein from the pairing with S100B and restore the biological function of p53 as a tumor suppressor. The analysis of the binding mode and ligand structural features would facilitate our effort to identify and design ligands to block S100B-p53 interaction effectively. The results from the work suggest that developing ligands targeting the interface of S100B and p53 could be a promising approach to recover the normal function of p53 as a tumor suppressor.

Keywords Protein interaction · EF-hand Ca^{2+} binding protein · Binding affinity calculation · Tumor suppressor · Anti-cancer agent · Drug development

Z. Zhou (✉)
Department of Medicinal Chemistry and Molecular Pharmacology, Purdue University, West Lafayette, IN 47907, USA
e-mail: zhou@pharmacy.purdue.edu;
zhou_zhigang@hotmail.com

Y. Li
Department of Chemistry, East Carolina University, Greenville, NC 27858, USA
e-mail: LIYU@ecu.edu

Introduction

S100 proteins are members of the dimeric EF Ca^{2+} binding family of proteins and have been found to play an important role in a wide range of biological signaling pathways [1–3]. Primarily found in glial cells, S100B is the prototype of the S100 family. Over expression of S100B proteins has been associated with a large spectrum of human diseases including Alzheimer's disease, Down's syndrome, cardiomyopathies, neurodegeneration, and cancer [4, 5]. More than 20 target proteins of S100B have been identified including the Alzheimer protein tau, neuromodulin, and tumor suppressor protein p53. p53 is a transcriptional activator and is frequently referred to as "The Guardian of the Genome" due to its tumor suppressing activities. p53 functions to stop the cell cycle, to prevent genetic alterations, and to induce apoptosis in response to the activation of certain oncogenes [6, 7]. S100B was observed in experiments to bind to the lower oligomerization states (monomer or dimer) of p53 [8–11]. p53 is active as a tumor suppressor only in its tetramer form; the binding of S100B disrupts the tetramerization equilibrium of p53 and prevents p53 from functioning [12, 13]. Such binding thus has a significant impact on cancer development [1, 14–21].

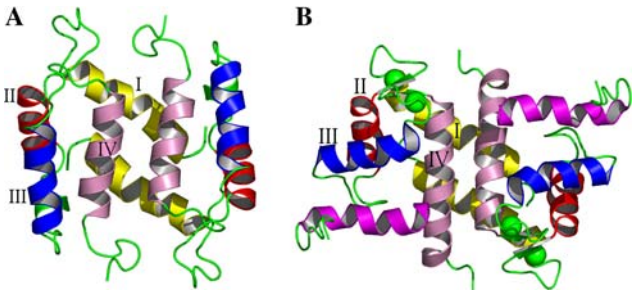

Fig. 1 The structures of S100B protein and its complex with p53. **a** Inactive form of S100B. **b** S100B and p53 (C-terminal) complex; The calcium ions are indicated as *green* spheres, S100B is colored based on domains (Domain I-*yellow*, domain II-*red*, domain III-*blue*, domain IV-*pink*), and p53 C-terminal peptides are in *magenta*

Three-dimensional structures of S100B and the complex with the C-terminal domain of p53 protein have been determined using NMR spectroscopy [9, 22, 23]. As shown in Fig. 1a, b S100B exists as a homodimer in solution and domain III undergoes significant conformational change upon binding with two calcium ions in the loop regions. Calcium binding to S100B induces a large conformational change and generates a hydrophobic surface (the grey in Fig. 1b) by changing the orientation of helix III and helix IV and placing helix III nearly perpendicular to helix IV and extending the helix IV by one turn [23]. Domain III turns about 90° relative to the other two domains between the two states. The conformation with calcium is the active form of S100B to bind to p53. The similarity between the calcium binding conformation and p53 binding conformation is high. No significant change is observed between the two states of S100B protein. The coordinates [9] of S100B complexed with p53 were used in this work to study the S100B-p53 interaction and the ligand with the potential to block the interaction by MD simulations. Potential ligands were identified using Glide docking simulations screened from the NCI library. The top compounds with the highest binding affinity to the interface of S100B-p53 and the highest potential to block the binding of p53 to S100B were selected for investigation using MD simulations.

Methods

Molecular structure preparation for screening

Ligands with the potential to bind to S100B and to block the association with p53 were screened from the NCI small molecular library (Diversity Library) using the Glide docking program. The NCI diversity library which comprises 1,990 compounds was used in the screening. The diversity small molecule library was selected with structural diversity based from approximately 140,000 compounds from NCI repository of synthetic and natural products sent to NCI to be evaluated as potential anticancer and anti-HIV agents over years (http://dtp.nci.nih.gov/docs/3d_database/Structural_information/structural_data.html). The reason that this molecule library was chosen is that chemical samples for the compounds in the library were available for anti-cancer research to experimentally evaluate the biological activity of selected compounds. Hydrogen atoms were added to each molecules and then the structure of each molecule was minimized using the OPLS-AA force field [24] implemented by the MOE program package (Chemical Computing Group) after partial charges were assigned based on the force field.

Protein coordinates were from the NMR solution structure of S100B-p53 complex (PDB ID: 1DT7) [9]. There is a small channel formed between the S100B and p53 protein which was used as the binding site to screen potential ligands being able to interfere with the interaction of the two proteins. Dummy atoms were added to the binding channel and minimizations were performed to optimize side chains and to enlarge the binding site. The preparation procedure resulted in a binding site $\sim$1 Å larger than the original one to mimic a dynamic vibration (breathing) of the protein complex in solution to let a ligand enter and bind through an induced-fit fashion, a common phenomenon occurring in many real-world ligand bindings under physiologic conditions.

The prepared protein coordinates were further processed following the Glide protocol for protein preparation by adding hydrogen atoms, assigning partial charges using the OPLS-AA force field and performing a small number of step minimizations to relax newly-added hydrogen atoms. The amino acids of each protein (S100B or p53) within 5 Å from the other one were selected to be treated as a binding site for ligand screening. The geometric center of the binding site was used as the center of the docking box used in the next section.

Molecular screening of chemical library by docking

A docking grid was generated with a center at the geometric center of the binding site described in the previous section. The binding site of the S100B protein was formed by helix **3** and **4**, at the binding interface of S100B with p53. A docking box with dimensions of 25 × 25 × 20 Å was used to allow the ligand to be docked into the pocket.

Compounds with less than 200 atoms and less than 35 rotatable bonds were docked into the defined docking box. All small molecules were treated as flexible molecules by generating possible rotamers by rotating each single bond torsion angle. The protein was treated as a rigid body in the grid generation step. The van der Waals (vdW) radii of heavy atoms were scaled down to 0.5 Å to allow larger

molecules to fit in the binding site with the purpose of accounting for some degree of reduced-fit effect. A limit of 5,000 poses per ligand was used to evaluate the binding score in the initial steps and the top 500 poses per ligand were subjected to energy minimization for further evaluation. Poses of a given molecule were output when the pose had more than 0.5 Å root mean square deviation (RMSD) in heavy atom coordinates and 1.0 Å of displacement for any one heavy atom. 5 poses for each molecule were recorded in the log file.

Compound selection

The empirical score, GlideScore (GScore), [25, 26] was used to rank and select compounds in docking simulations. Based on our experience in our screening, Gscore produced better results than Emodel. Gscore was used to rank docked poses and compounds [27]. The extra-precision (XP) of the docking protocol was used in docking screening. The top 200 compounds were selected from the screening and were subjected to complex structure relaxation. The receptor–ligand complex relaxation was fulfilled using energy minimization with Liaison Module (FirstDiscovery suite) [28, 29]. All ligand atoms and the protein atoms within 9 Å of any ligand atom were relaxed while all other protein atoms were fixed. Liaison Module was developed to calculate binding energies and establish a linear response energy equation for known activity of a set of compounds. The first part of the function of Liaison that relaxes receptor/ligand complex structure and calculates the energy terms was used in the work to calculate the binding energy based on the OPLS-AA force field [24]. The energy includes electrostatic, van de Waals, and solvation energy terms. Solvation was modeled implicitly using the surface generalized Born (SGB) model which includes the solvent reaction-field energy, U_{rxnf} and the cavity energy, U_{cav}, proportional to the change in exposed surface area of the ligand. Energy minimization was carried out for 500 steps, or until the system reached a root-mean-square (rms) gradient of less than 0.01. The final top 10 compounds were selected based on the binding energy for visual examination of the interaction mode with the proteins.

MD simulation

Based on the structures determined by the docking simulations, molecular dynamics simulations were carried out using AMBER8 for the complexes of S100B and p53 with or without the selected ligands, and for the complexes of S100B and the selected ligands. The three-dimensional structure of the complex of S100B and the C-terminal peptide of p53 (Fig. 1b, 1DT7.pdb) includes 22 residues from the C-terminal domain of p53, 184 residues of S100B and four calcium ions. All structures were neutralized with counter ions (Cl^-), and explicitly solvated using TIP3P water in an octahedral water box.

The structures of the organic molecules were optimized using semi-empirical AM1 method using MOPAC6 package. The partial charges for organic molecules were fitted from the calculated charges based on AM1 calculations through the Antechamber module of AMBER.

The particle mesh Ewald (PME) method was used to treat long-range electrostatic interactions, with a cubic B-spline interpolation. A cutoff of 8.0 Å (default) was used to limit direct space sum in PME. SHAKE was used to constrain all bonds involving hydrogen atoms with a geometric tolerance of 0.00001 Å. A cutoff of 9 Å was used for vdW non-bonded interactions. Periodic boundary conditions were used. A time step of 1 fs was used for the equilibration simulation and 2 fs were used for production simulation. The temperature was rescaled with the Berendsen weak-coupling algorithm, [30] with a time constant of 0.5 ps for the heat bath. After the system was heated to 300 K from the initial temperature of 100 K, molecular dynamics were performed at a constant temperature of 300 K.

Prior to production MD simulation, three steps of energy minimization were carefully carried out to relax (1) hydrogen atoms, (2) side chains and (3) all atoms. Then the system was gradually heated to 300 K and relaxed for 500 ps using constant pressure (NPT) molecular dynamics (MD) simulation as an equilibration simulation. The density and other properties of the system were examined to ensure that the system was ready for production simulation. The production simulation was carried out using NPT ensemble.

Binding energy calculation by MMPBSA

The free energy of the ligand binding in the non-nucleotide inhibitor binding pocket was analyzed by the Molecular Mechanics-Poisson Boltzmann Surface Area (MM-PBSA) method [31–33], integrated in AMBER8. The binding free energy was calculated as the average of the binding free energy of the 500 snapshots, taken from the trajectories of each simulation. The free energy was calculated as:

$$\Delta G_{\mathrm{tot}} = \Delta E_{\mathrm{MM}} + \Delta G_{\mathrm{sol}} - T\Delta S \quad (1)$$

where ΔE_{MM} is the molecular mechanics energy, comprised of a vdW and an electrostatic contribution; ΔG_{sol} is the solvation energy, which consists of electrostatic and nonpolar interactions. The electrostatic solvation energy is determined using the finite difference Poisson–Boltzmann method and the nonpolar contribution is estimated by the solvent-accessibility surface method. $T\Delta S$ is the entropy contribution to the free energy, which is estimated using

normal mode analysis. The purpose of the work is to compare the relative binding energy of the same molecular system with slight differences in binding structure. The variance of entropy contributions for different systems was assumed to be very small due to the terms cancelling out when comparing energy levels. So the calculation of entropy was omitted to save time on the time-consuming step. The same force field used in the MD simulations was used in the free energy calculations. The binding free energy for the ligand in a protein can be estimated using:

$$\Delta G_b = \Delta G_c - (\Delta G_p + \Delta G_l) \quad (2)$$

where c, p and l denote the protein/ligand complex, the protein and the ligand, respectively.

Results and discussion

Identification of potential ligands

According to the screening strategy described in the "Methods" section, docking simulations were carried out to screen potential ligands from the NCI Diversity Library against the pocket at the interface between S100B and p53 proteins. The Diversity Library contains about 1,990 compounds selected from a larger set of compounds tested at NCI. As found in our previous study [34], Gscore performed better than other scoring functions available to Glide to rank active compounds in the Glide docking screening. So, only Gscore was used to rank compounds in this work. The plot of Gscore for the compounds from the screening is depicted in Fig. 2. The Gscore decreases rapidly for the first 50 compounds, then decreases slowly until approximately compound 1,000, and again decreases rapidly to approach zero (0). The 250 molecules with the highest GScore were selected as top molecules and the complexes of these compounds with protein were further refined by energy minimization carried out with the Liaison module. The calculated Liaison binding energy was used to rank the compounds. Such hierarchy approach consisting Gscore-ranking from GLIDE docking and Liaison binding energy-ranking from complex minimization is an efficient and effective way to select top compounds from a molecule library in silico screening [34]. The bound structures of the top 10 compounds in S100B-p53 were visually examined and the compounds which have the strongest potential to interfere with the interaction of the two proteins were selected as potential ligands. Three compounds were selected for further investigation of ligand-binding effect on the protein interaction of S100B and p53 by MD simulation. The structures of the three selected compounds are listed in Fig. 3. Two compounds feature two ring groups linked by a single bond chain. The third compound contains three fused planar rings plus one linked aromatic ring and a chain tail.

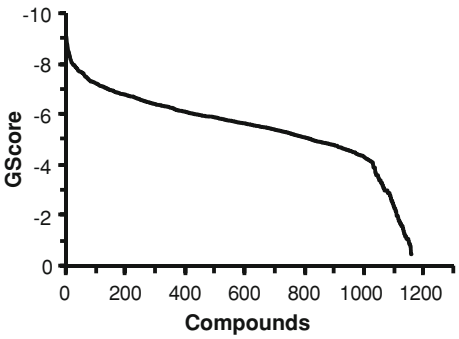

Fig. 2 The plot of ligand GScores from the high throughput docking screening

The bound structures of the three compounds are depicted in Fig. 4. The bound structures show that the three compounds bind just between S100B (red) and p53 (magenta) (Fig. 4a, c) and that p53 covers most parts of the compounds (Fig. 4b, d). The binding site of S100B is mainly formed by domain II (helix in red), III (helix in blue), and IV (helix in pink) (Fig. 4c, d). The compounds have proper contacts (direct interactions) with the protein (Fig. 4a), which suggests that they can bind well to S100B before p53 binds to the protein. It is seen that the three compounds mainly block the direct interaction of p53 with domain II and III of S100B. In addition, compound 3 also partially blocks the direct interaction of p53 with domain IV of S100B (Fig. 4c, d).

Based on the docked structures, it is noticed that hydrogen bonds can be formed between compounds and amino acids E45, T59, Q71, and K111 (Fig. 5). Compound **1** has hydrogen bond interactions with amino acids E45 and T59. Compound **3** has hydrogen bond interactions with amino acids T59, Q71, and K111. The hydrogen bond interaction (polar) plays an important role in ligand binding and in the recognition of binding modes and has a contribution to the binding affinity. Also it can be observed in the figure that most parts of the protein surface on the binding site are hydrophobic (green colored). The compounds have hydrophobic aromatic rings which have direct contact with the hydrophobic protein surface. Thus, hydrophobic interaction is also an important element for the binding of these compounds in the hydrophobic binding site.

MD simulation of the protein complexes

The five proteins or proteins–ligand molecular systems were simulated using MD simulations to study the effect of ligand binding to the protein–protein interaction. The structural behaviors and energetic features of protein–

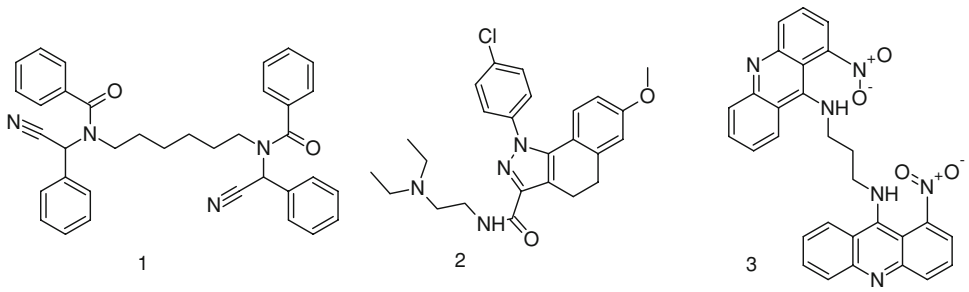

Fig. 3 The molecular structures of three selected compounds. **1** (681, CID **387715**); **2** (288, CID **5351294**); 3 (690, CID **391439**)

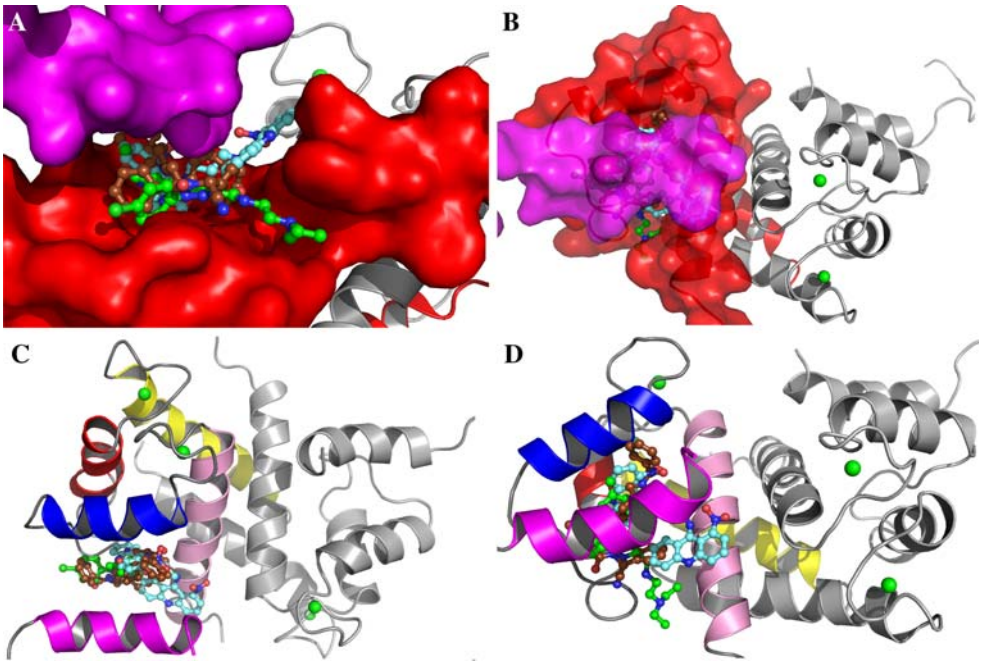

Fig. 4 The bound structures of the three compounds in S100B-p53 protein complex. The superposition of three compounds show that they bind in the binding interface between S100B (represented in *red* surface in **a** and **b** and variable colors in **c** and **d**) and p53 (colored in *magenta*) and have potential to interfere with the binding of the two proteins. Carbon atoms of compound **1**, **2**, and **3** are colored in *brown*, *green*, and *cyan*, respectively. Oxygen atoms are colored in *red* and nitrogen atoms are colored in *blue* for the three compounds. **a**, **b** the S100B and p53 complex is depicted with surface of S100B in *red* and p53 in *magenta*. The other S100B in the dimer is shown within the *cartoon* and is shaded *grey*. **a** is *side view* and **b** is *upside down*. **c** and **d** the S100B and p53 proteins are shown in *cartoon* and the compound bound in the interface are shown in *stick-ball* modes

protein interaction were further analyzed based on the snapshots taken from the molecular trajectories of MD simulations.

The system energy in simulations was checked to see if each molecular system remains energetically stable. The plots of the total energy for the 5 simulations are depicted in Fig. 6. It is observed that the total energy for all 5 molecular systems remains stable with some degree of fluctuation after 2 ns of simulation. An energetic stability of the molecular system has been observed for each molecular system after the 2 ns simulation. All of the following analysis were carried out based on the stability of the simulation after the 2 ns of equilibration.

Based on the atomic position fluctuations (APF) of the protein (Fig. 7) calculated based on the 500 snapshots taken from the trajectories of the last 7 ns of the simulations, it was noticed that the resides with well defined structures (helix regions) have very small APF (<1 Å), which means the structural fluctuations are very small for these helices and the whole protein (APF was calculated based on the superimpositions of all of the alpha carbon atoms). On the other hand, the C-terminus and N-terminus of the chains have very large APF. These termini are very flexible, especially the N and C-termini of chain 3 and 4 (p53). All the 5 molecular systems have a very similar level and pattern of APF. The overall conformation change is not large based on the 1 Å APF for helixes. The stability of the whole protein structure makes it possible to obtain reliable analysis on ligand binding and its effect on protein-protein interaction through MD simulation.

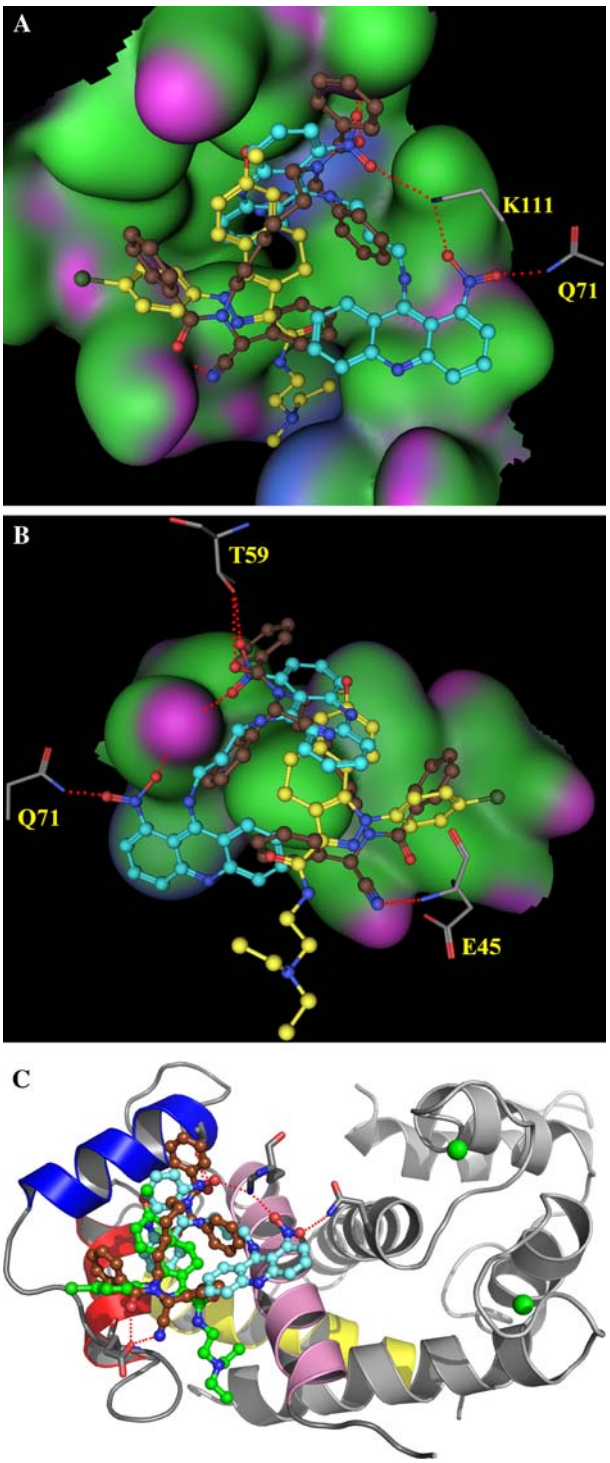

Fig. 5 The surface properties of the S100B and p53 at the interface where the three compounds bind and the hydrogen bonds just form between the compounds and amino acids of the proteins. The hydrophobic part is colored in *green*, the hydrogen bond forming part is colored in *magenta*, and the mild-hydrophilic part is colored in *blue*. The hydrogen bonds are marked with *red doted lines*. Carbon atoms of compound **1** and **3** are colored in *brown* and *cyan*, respectively. Carbon atoms of compound **2** are colored in *yellow* in **a** and **b** and in *green* in **c**. Oxygen atoms are colored in *red* and nitrogen atoms are colored in *blue* for the three compounds

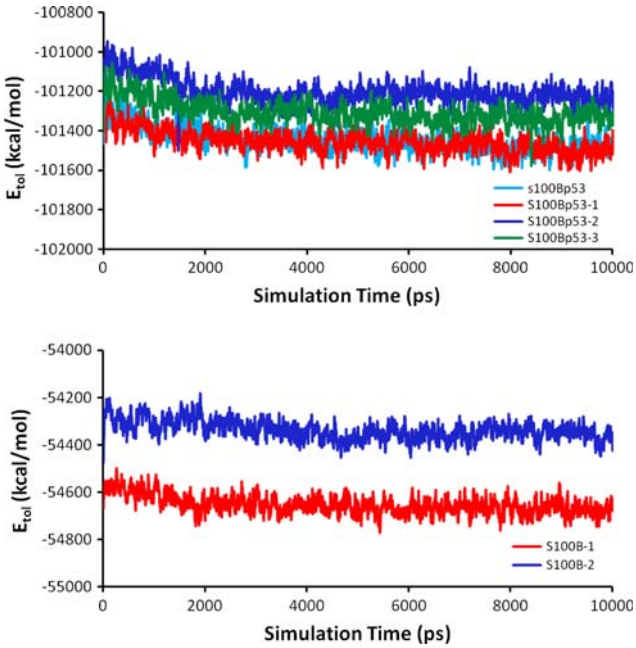

Fig. 6 The plots of the total energy of MD simulation. The *upper panel* is for the S100Bp53 protein and the complexes with compound **1**, **2**, and **3**. The *lower panel* is for the S100B protein complexes with ligand **1** and **2**. The energies remain stable after about 2 ns of simulations. *Legends* S100Bp53: the complex of S100B and p53 proteins; S100Bp53-1, S100Bp53-2, and S100Bp53-3: the complex of S100Bp53 protein with compound **1**, **2**, or **3**, respectively; S100B-1 and S100B-2: the complex of S100B protein with compound **1** or **2**, respectively

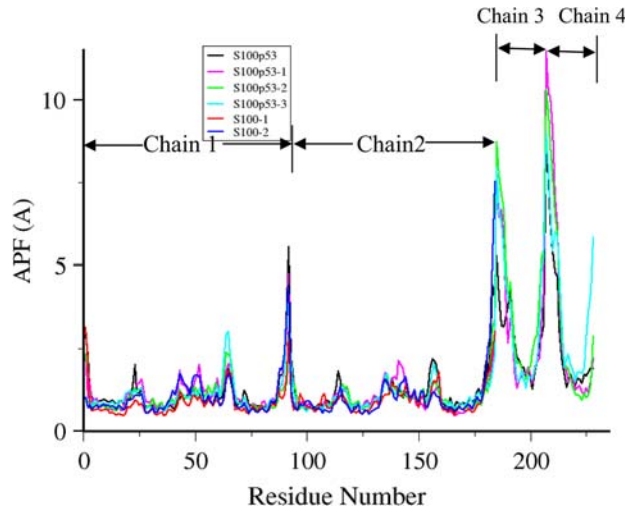

Fig. 7 The atomic position fluctuation from the simulation of S100B complex with NCI ligand. During the simulations, the parts with well-defined structures have small fluctuations (<2 Å). The most flexible parts are the tails of the four chains. All 6 simulations have very similar plots. *Legends* S100Bp53: the complex of S100B and p53 proteins; S100Bp53-1, S100Bp53-2, and S100Bp53-3: the complex of S100Bp53 protein with compound **1**, **2**, or **3**, respectively; S100B-1 and S100B-2: the complex of S100B protein with compound **1** or **2**, respectively

Ligand binding interference on S100B-p53 interaction

With the purpose to evaluate the ligand binding effect on the protein-protein interaction of S100B and p53, we examined the distance between the key parts of the protein which reflects the interaction of S100B and p53. The plots of the distances between some keys residues are shown in Fig. 8. The distance (Fig. 8a) between residues (amino acids V52-Q57) of S100B domain III and the residues (amino acids R104-F111) of p53 shows that the distances between of the ligated S100B-p53 complexed with compound **1** or **2** are larger than that of the unligated protein complex (S100B-p53). The results indicate that the ligand propels the two proteins apart for about 2 Å when it binds to the binding interface of the proteins. With the increase of the protein distance, the interaction of the proteins will decrease. For the S100B-p53-compound 3 complex, the distance keeps roughly the same with the distance of the unligated S100B-p53 complex from the beginning to approximately 8 ns. After that, the distance of the ligated system increases.

By checking the distance between the residues (amino acids E72–T81) of domain IV and the residues (amino acids M109-T112) of p53, we notice that the distances for two ligated complexes (S100B-p53-compound **1** and S100B-p53-compound **3**) are larger than that of the unligated complex (S100B-p53). The distance for the ligated S100B-p53-compound **2** complex is roughly the same as that of the unligated complex. Together with previous results, we can observe that the bound compound **1** pushed p53 away from domain III and IV of S100B, while the bound compound **2** propelled p53 away just from domain III and bound compound **3** drove p53 away only from domain IV of S100B in the MD simulations. What happened is characterized by the cartoon shown in Fig. 8e. Checking the bound structures and the molecular structures shown in Figs. 4 and 5, we can see that compound **1** is relatively bulky in the binding site and it is understandable

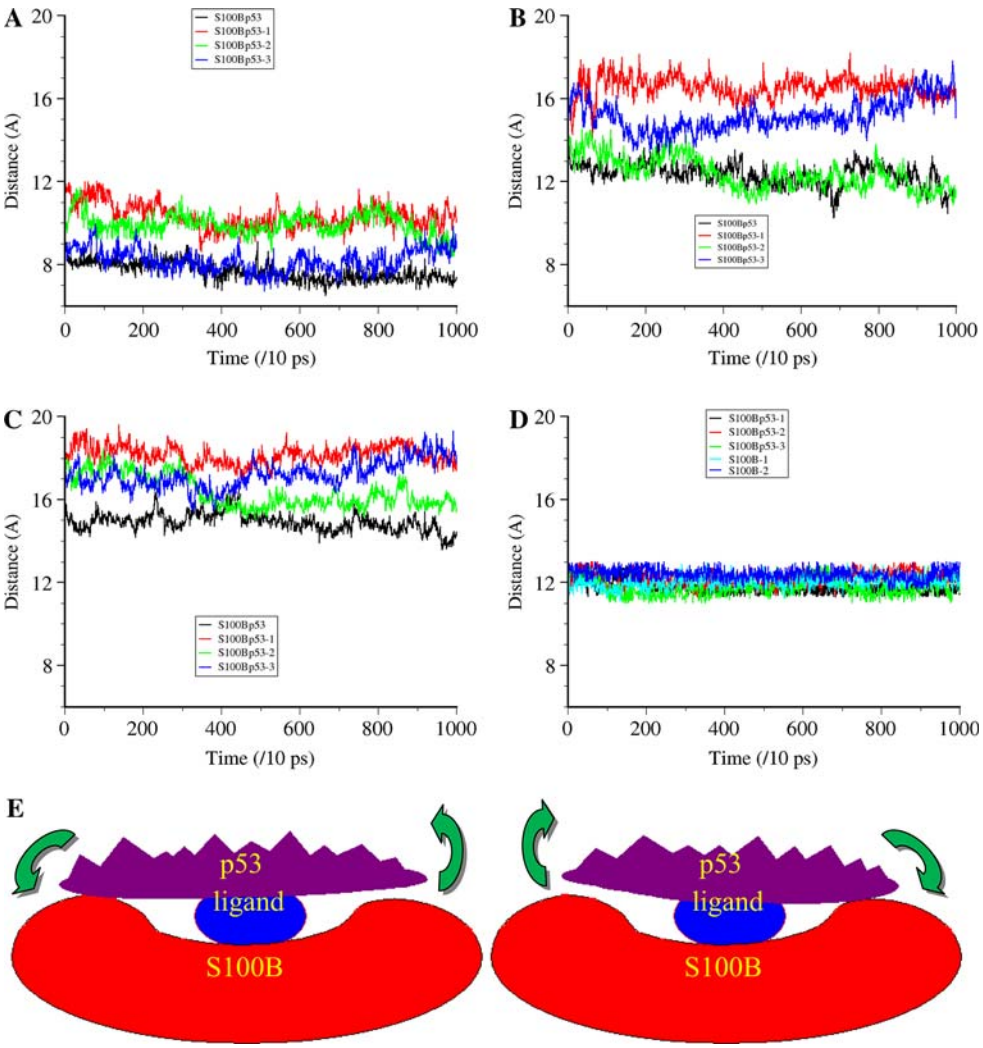

Fig. 8 The plots of the distance between the interested chains, domains, and ligands during simulation. The distances were calculated based on the geometric centers of the alpha carbon atoms of a set of selected residues as indicated below for each *panel*. **a** The distance between domain III (amino acids V52-Q57) of S100B and p53 (amino acids R104-F110). **b** The distance between domain IV (amino acids E72-T81) of S100B and p53 (amino acids M109-T112). **c** The distance between chain 1 (p53) and chain 3 (S100B). **d** The distance between chain 1 and ligand compound. *Legends* S100Bp53: the complex of S100B and p53 proteins; S100Bp53-1, S100Bp53-2, and S100Bp53-3: the complex of S100Bp53 protein with compound **1**, **2**, or **3**, respectively; S100B-1 and S100B-2: the complex of S100B protein with compound **1** or **2**, respectively. **e** The schematic illustration shows the two interaction formats of S100B and p53 affected by ligand binding

that this compound has the potential to push the whole p53 helix away from S100B. The bound compound **2** is more away from domain IV than the other two compounds, so the compound should have the least impact on the interaction of p53 with domain IV among all three compounds. On the other hand, part of compound 2 is located just between p53 and domain IV of S100B. This compound should have the highest impact to the interaction of p53 and domain IV. The features on molecular and bound structures are consistent with the observations obtained from MD simulation based on the distance changes.

The distance between p53 and chain 1 (one S100B in the dimer) of S100B is shown in Fig. 8c. The distances of all three ligated complexes are larger than that of unligated S100B-p53 complex. Between the distance between S100B and p53 of compound **1**, S100B-p53-complex is the largest, that of the compound **3** complex is the second, and that of compound **2** complex is the smallest. This result indicates that, when it binds to the interface of the two proteins, a ligand will interfere with the interaction of the two proteins by pushing them away from each other for some distance compared to the equilibrium state of the unligated proteins. The weakened interaction between the two proteins upon ligand binding could result in protein dissociation and have consequences on the biological activity of the proteins which are affected by protein association. The findings based on the distance analysis are further supported by the binding affinity evaluation discussed in the next section.

If a ligand is able to bind to free S100B stably, it could prevent p53 from binding to S100B. The binding stability of the two ligands to S100B was examined by comparing with the three compounds binding to S100B-p53 complexes using the MD simulations. The simulation results of S100B-ligand complex show that the two ligands can bind stably to S100B alone during the simulations. The distances between ligand and S100B (chain 1) for the three S100B-compound complexes are displayed in Fig. 8d. It is found that the distances between each compound and S100B (chain 1) keep flat and are very similar to each other. Comparing the same compound in S100B complex and in S100B-p53 complex, it is observed that the distances in two complexes are very close to each other. The two curves for the same compounds in different proteins fluctuate roughly along the same base line, which represents the average distance between the ligand and the protein. For example, the distances between compound **1** and S100B in free S100B (cyan curve) and in S100B-p53 complex (black curve) are very close to each other and it is also true for compound 2 (blue curve vs. red curve in Fig. 8d). This result shows that the three ligands are able to bind to free S100B protein at the p53 binding site stably and as tightly as they bind to S100B-p53 complex. Such ligand binding could prevent p53 from binding to S100B.

Free energy of binding calculation

The free energy of binding between S100B and p53 was calculated using the MM-PBSA approach from AMBER based on the 500 snapshots taken from the trajectory of the last 7 ns simulation to estimate the binding affinity of the two proteins. For the purpose of comparison of relative binding affinity of the two same proteins in slightly different binding conditions, we reasonably assume that the entropy contribution to the free energy of binding would be very similar and can be cancelled out in comparison. To save computational time, the very time-consuming entropy calculation was omitted. This binding energy is a reasonable way to evaluate the relative binding affinity of the two same proteins in slightly different conditions. The calculated average energies for each binding energy term of S100B/p53 proteins and S100B/ligand are listed in Table 1. For the S100B and p53 interactions, the ligand

Table 1 The calculated binding energy in kcal/mol from MMPBSA method based on the last 500 snapshots taken from the trajectories of the 10 ns simulation for each of the complexes

Complex system	E_{ele}		E_{vdW}		E_{sol}		ΔG
	Mean	SD	Mean	SD	Mean	SD	
S100Bp53m	−595.01	63.22	−54.22	7.20	610.98	61.11	−38.25
S100Bp53m211	−564.32	53.82	−37.52	12.07	572.14	58.41	−29.70
S100Bp53m288	−567.07	68.64	−17.74	3.29	561.19	65.66	−23.63
S100Bp53m690	−524.90	35.31	−29.65	4.91	527.21	33.67	−27.34
S100B-211	−14.89	7.80	−35.57	2.99	8.47	4.87	−41.99
S100B-288	−22.29	9.28	−32.78	3.22	15.30	6.88	−39.77
S100B-690	−20.72	9.33	−38.28	3.39	18.16	7.42	−40.83

E_{ele} and E_{vdW} are the electrostatic and vdW contribution to the binding energy calculated from force field, respectively. E_{sol} is the solvation contribution to the binding energy calculated using PBSA implicit water model. $\Delta G = E_{ele} + E_{vdW} + E_{sol}$

SD standard deviation

compound and water were not included in the energy calculations. For the S100B and ligand interactions, the p53 and water were excluded from the energy calculations. For gas phase energies, the electrostatic and solvation energies are much larger than vdW energy, but with opposite signs. The similar magnitudes with opposite signs mean that the two energies work in opposing directions and were cancelled out. The electrostatic energy is favorable for the association of the two proteins and has positive effects on the binding, while on the other hand; the solvation energy is unfavorable for the association and has negative effects on the binding process for all four (4) systems. The vdW energy is the major contribution to the binding. The association of the two proteins is probably driven by vdW interaction. The calculated binding energy (ΔG) shows that the S100B-p53 system has the larger binding energy (lower in negative) for the two proteins than all three ligated complexes (S100B-p53-compound **1**, **2**, and **3**). The energy difference between the unligated S100B-p53 system and the ligated S100B-p53-ligand (**1**, **2**, and **3**) ranges from -8.5 to -14.6 kcal/mol. S100B and p53 have stronger interactions in the unligated S100B-p53 complex than the ligated complexes. The results show that ligand binding significantly weakens the interaction of S100B and p53 and thermodynamically favors dissociation over association of the two proteins. The calculated binding energies of three ligands to S100B were from -39.77 to -41.99 kcal/mol, which are slightly higher than the binding energy of S100B and p53. With consideration of the level of standard deviation (STD) of the calculations, such difference in the binding energies between S100/p53 and S100/ligand is not statistically significant. So, the results indict that these three ligands can bind to S100 with the same level of affinity or higher than p53 does and the ligands can compete to bind to S100 with p53. Such ligand binding disturbs the normal association of S100B and p53. Through the shift of the S100B-p53 association/dissociation equilibration, more free p53 will be available to execute its normal biological function, as a tumor suppressor.

Conclusion

This work indicated that a ligand binding at the interface of S100B with p53 has the potential to interfere with the interaction of the two proteins.

Compounds with the potential to bind at the interface of S100B and p53 were screened from a small molecule library using HTS docking simulation. Two steps of screening were carried out to identify the top potential compounds. Three compounds were selected based on their binding energies and their binding modes to the binding site for further examination of our hypothesis. The bound structures of the compounds show that they have great potential to interfere with the interaction of the two proteins as they bind in the heart of the binding interface of the two proteins.

The MD simulations of the protein-ligand (S100B-p53-ligand) complexes for the three selected compounds show that ligands binding in the interface were able to push the two proteins apart for a certain distance compared to the unligated S100B-p53 complex. The three compounds propelled p53 away from S100B in different ways depending on ligand size and their binding modes to the interface. The observation of ligand effects on the protein dissociation is consistent with the analysis on ligand structure features and binding modes. The calculated binding energy results show that the binding affinity of p53 and S100B of the three ligated complexes is apparently lower (higher negative value) than that of the unligated S100B-p53 complex. This is consistent with the observations of the distances which measure the direct contact of S100B and p53; S100B and p53 have looser contact in ligated complexes than in the unligated complexes. Based on the binding energy calculation, it is noticed that vdW energy could be the major force in the binding.

The stability of ligand binding to the free S100B and the binding energy of the ligands to S100B were evaluated by MD simulations and compared with the binding to the S100B-p53 complex. The results demonstrated that the compounds are able to bind to free S100B as strongly as (or stronger than) p53 does and as stably as to S100B-p53 complex. This indicated that such ligands have the potential to bind to the free S100B and then prevent p53 from binding to S100B. The shift on the equilibration to the dissociation of S100B and p53 will free more p53 from forming complex with S100B. The availability of p53 will restore the protein's normal biological function which is suppressed by S100B association. The interference and blockage of S100B interaction with p53 could have important consequences to recover the biological function of p53 as a tumor suppressor. The interaction features analyzed in this study will facilitate our effort to identify and design ligands to block the interaction effectively.

Acknowledgments This work was partially supported by Research Corporation Cottrell College Science Awards (CC6786), East Carolina University 2005 Research/Creativity Activity Grant, East Carolina 2007–2008 Research Development Award. The authors thank the developers of Pymol software for sharing the program to prepare the molecular figures used in the paper.

References

1. Donato R (2001) Int J Biochem Cell Biol 33:637
2. Heizmann CW (1999) Neurochem Res 24:1097
3. Heizmann CW, Fritz G, Schäfer BW (2002) Front Biosci 7:1356
4. Baudier J, Glasser N, Gerard D (1986) J Biol Chem 261:8192

5. Odink K, Cerletti N, Brüggen J, Clerc RG, Tarcsay L, Zwadlo G, Gerhards G, Schlegel R, Sorg C (1987) Nature 330:80
6. Levine AJ (1997) Cell 88:323
7. Oren M (1999) J Biol Chem 274:36031
8. Fernandez-Fernandez MR, Veprintsev DB, Fersht AR (2005) Proc Natl Acad Sci USA 102:4735
9. Rust RR, Baldisseri DM, Weber DJ (2000) Nat Struct Biol 7:570
10. Grigorian M, Andresen S, Tulchinsky E, Kriajevska M, Carlberg C, Kruse C, Cohn M, Ambartsumian N, Christensen A, Selivanova G, Lukanidin E (2001) J Biol Chem 276:22699
11. Markowitz J, Rustandi RR, Varney KM, Wilder PT, Udan R, Wu SL, Horrocks WD, Weber DJ (2005) Biochemistry 44:7305
12. Halazonetis TD, Kandil AN (1993) EMBO J 12:5057
13. Hainaut P, Hall A, Milner J (1994) Oncogene 9:299
14. Deichmann M, Benner A, Bock M, Jäckel A, Uhl K, Waldmann V, Näher H (1999) J Clin Oncol 17:1891
15. Hauschild A, Michaelsen J, Brenner W, Rudolph P, Gläser R, Henze E, Christophers E (1999) Melanoma Res 9:155
16. Berridge MJ, Bootman MD, Roderick HL (2003) Nat Rev Mol Cell Biol 4:517
17. Ebralidze A, Tulchinsky E, Grigorian M, Afanasyeva A, Senin V, Revazova E, Lukanidin E (1989) Genes Dev 3:1086
18. Lloyd BH, Platt-Higgins A, Rudland PS, Barraclough R (1998) Oncogene 17:465
19. Davies M, Rudland P, Robertson L, Parry E, Jolicoeur P, Barraclough R (1996) Oncogene 13:1631
20. Davies B, Davies M, Gibbs F, Barraclough R, Rudland P (1993) Oncogene 8:999
21. Ambartsumian N, Grigorian M, Larsen I, Karlstrøm O, Sidenius N, Rygaard J, Georgiev G, Lukanidin E (1996) Oncogene 13:1621
22. Drohat AC, TJandra N, Baldisseri DM, Weber DJ (1999) Protein Sci 8:800
23. Drohat AC, Baldisseri DM, Rustandi RR, Weber DJ (1998) Biochemistry 37:2729
24. Jorgensen WL, Maxwell DS, Tirado-Rives J (1996) J Am Chem Soc 118:11225
25. Friesner RA, Banks JL, Murphy RB, Halgren TA, Klicic JJ, Mainz DT, Repasky MP, Knoll EH, Shelley M, Perry JK, Shaw DE, Francis P, Shenkin PS (2004) J Med Chem 47:1739
26. Friesner RA, Murphy RB, Repasky MP, Frye LL, Greenwood JR, Halgren TA, Sanschagrin PC, Mainz DT (2006) J Med Chem 49:6177
27. Zhou Z, Khaliq M, Suk J-E, Patkar C, Li L, Kuhn RJ, Post CB (2008). ACS Chem Biol 3:765–775
28. Rizzo RC, Tirado-Rives J, Jorgensen WL (2001) J Med Chem 44:145
29. Kroeger Smith MB, Hose BM, Hawkins A, Lipchock J, Farnsworth DW, Rizzo RC, Tirado-Rives J, Arnold E, Zhang W, Hughes SH, Jorgensen WL, Michejda CJ, Smith RH Jr (2003) J Med Chem 46:1940
30. Berendsen HJC, Postma JPM, Van Gunsteren WF, DiNola A, Haak JR (1984) J Chem Phys 81:3684
31. Wang J, Morin P, Wang W, Kollman PA (2001) J Am Chem Soc 123:5221
32. Wang W, Kollman PA (2000) J Mol Biol 303:567
33. Kollman PA, Massova I, Reyes C, Kuhn B, Huo S, Chong L, Lee M, Lee T, Duan Y, Wang W, Donini O, Cieplak P, Srinivasan J, Case DA, Cheatham TEIII (2000) Acc Chem Res 33:889
34. Zhou Z, Patkar C, Li L, Kuhn R, Post CB (2008) ACS Chem Biol 3:765